CHAPTER 6

EVOLVING ELONGATED PULSAR BEAMS

6.1 INTRODUCTION

In this chapter we will attempt to resolve the most important uncertainty in our birthrate calculation, viz., the beaming fraction f which depends upon the shape and size of the pulsar beam* Most current theories of pulsar electro-dynamics implicitly assume that the pulsar beam is a cone of circular cross-section, particularly when they are dealing with a dipole magnetic field geometry, We discuss here a strong inconsistency between this assumption and the currently available polarization data on pulsars, Before proceeding further, we will briefly outline the essentials of the polarization model proposed by Radhakrishnan and Cooke (1969; henceforth RC) (based on their early observations on the Vela pulsar), the main elements of which underlie most current pulsar theories,

In the RC model the source of radiation is believed to be in the vicinity of a magnetic pole. Charged particles are accelerated along the open field lines emanating from the polar region (Goldreich and Julian 1969) and these emit radio-frequency curvature radiation in the direction of their motion. Since curvature radiation is beamed tangential to the magnetic field, the radiation forms a hollow conical beam (Komesaroff 1970) directed radially outward from the star and centred on the magnetic axis, and different parts of the pulse are emitted from different parts of the polar cap. Curvature radiation is polarized parallel to the plane of curvature of the magnetic field and hence the polarization angle variation within the pulse maps the orientation of the projected magnetic field at various points in the line of sight within the pulsar beam. On the basis of the simple polarization angle variation observed in PSR 0833-45, Radhakrishnan and Cooke (1969) proposed that the magnetic field at the radiation source is essentially dipolar so that the field lines are radial when projected on a plane perpendicular to the magnetic axis (fig. 6.1) Many later polarization studies (Manchester and Taylor (1977), and notably Backer and Rankin (1980) have strongly favoured the RC picture.

Figure 6.1 shows that, if 2θ is the total polarisation angle swing across the pulse, then for a beam of circular cross-sect ion,

$$\cos\theta = |y/r| \tag{6.1}$$

where y is the. latitude off-set between the line of sight and the magnetic pole and r is the radius of the beam.* If pulsars are oriented randomly with respect to Earth, then we expect $|y/r|$ to be uniformly distributed between 0 and 1 (neglecting

*The radius depends upon the definition of the boundary of the beam, Throughout this chapter we define the periphery as that point at which the 400 MHz radio flux falls to 10% of the pulse peak,

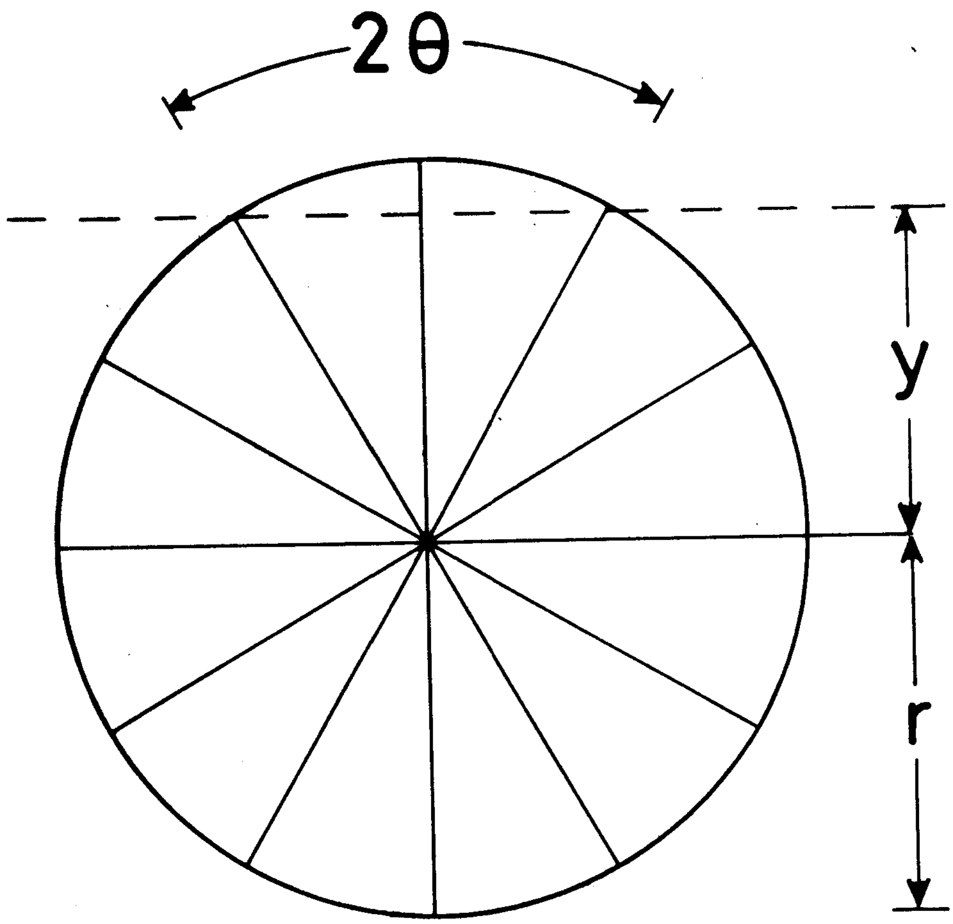

FIG. 6.1 Schematic representation of a circular pulsar beam of radius r. In the RC model, the projected magnetic field lines are taken to be radial, as shown. The dashed line is the path taken by a typical line of sight at the offset y from the beam centre. The total swing 2 8 of the position angle of the linearly polarised component of the radio radiation is determined entirely by the ratio $|y/r|$ (neglecting the spherical nature of the problem).

selection and spherical effects for the moment, which means that $y_{\cdot}, + \ll \pi/2$). Table 6.1 lists values of 2θ for 16 pulsars (from the observations of Backer and Rankin 1980) and shows a serious discrepancy. Equation (6.1) implies that half the pulsars should have 2θ values greater than 120^o $(=2\cos^{-1}(0.5))$ whereas only 3 out of 16 pulsars show this* Further, 4 out of 16 pulsars ought to have 2θ values less than 82.8^o but table 6.1 lists 11; 2 pulsars should have $2\theta < 57.9^o$ but there are 8; only 1 pulsar should have $2\theta < 40.7^o$ but there are 6; etc. There is clearly a massive discrepancy between the observations and the predictions of the simple RC model* It is obvious that no ordinary selection effect can explain the differences (we discuss this question in greater detail later), For instance the data in table 6.1 suggest that half the observed pulsars correspond to lines of sight intersecting the outer one-eighth of the circular beam. This is unlikely since all available evidence (including the arguments in section 6.5) point to a beam luminosity (and pulsar visibility) that falls away from the centre.

It is possible to argue that, because of the large discrepancy discussed above, the RC model is wrong in all respects* However, compelling observational evidence has accumulated in favour of many aspects of the model (e.g., Manchester and Taylor 1977). In this chapter we show that all that is needed is to abandon the circular beam hypothesis. The observations are consistent with the key features of the RC mode\ such as (1) radiation from magnetic poles, (2) dipolar field geometry, and (3) polarisation position angle related to projected field direction, provided we allow for an elongated beam cross-section (in addition to eliminating orthogonal modes as suggested by Packer and Rankin (1980)). To obtain numerical estimates of the elongation we assume the shape of the beam to be an ellipse* which is the most direct generalization of a circle (this leads to a conservative estimate of the beam elongation as discussed in section 6.3).

6.2 THEORY

We assume that pulsar beams are elliptical in shape with the principal axes oriented East-West and North-South with respect to the rotation axis; i.e., parallel to the local lines of constant longitude and constant latitude respectively* Let the dimension of. the semi-axis in the North-South direction be Y and let it be Y/R in the perpendicular direction (fig. 6.2). We are interested in estimating the elongation parameter R , which we initially take to be the same in all pulsars in a given sample.

As the pulsar rotates, the line of sight to Earth traces an East-West line on the pulsar beam, i.e., a line of constant latitude (fig. 6.2). If y is the off-set between the line of sight and the magnetic pole, then the total polarisation swing 2θ for an elliptic beam in the RC model can be obtained from

$$\cos\theta = R\,|y/Y|\left[1 + (y/Y)^2 (R^2-1)\right]^{-1/2} \qquad (6.2)$$

We are here neglecting the spherical effects which are treated in detail in section 6.5. Let us assume that there is equal probability of observing pulsars anywhere within the range

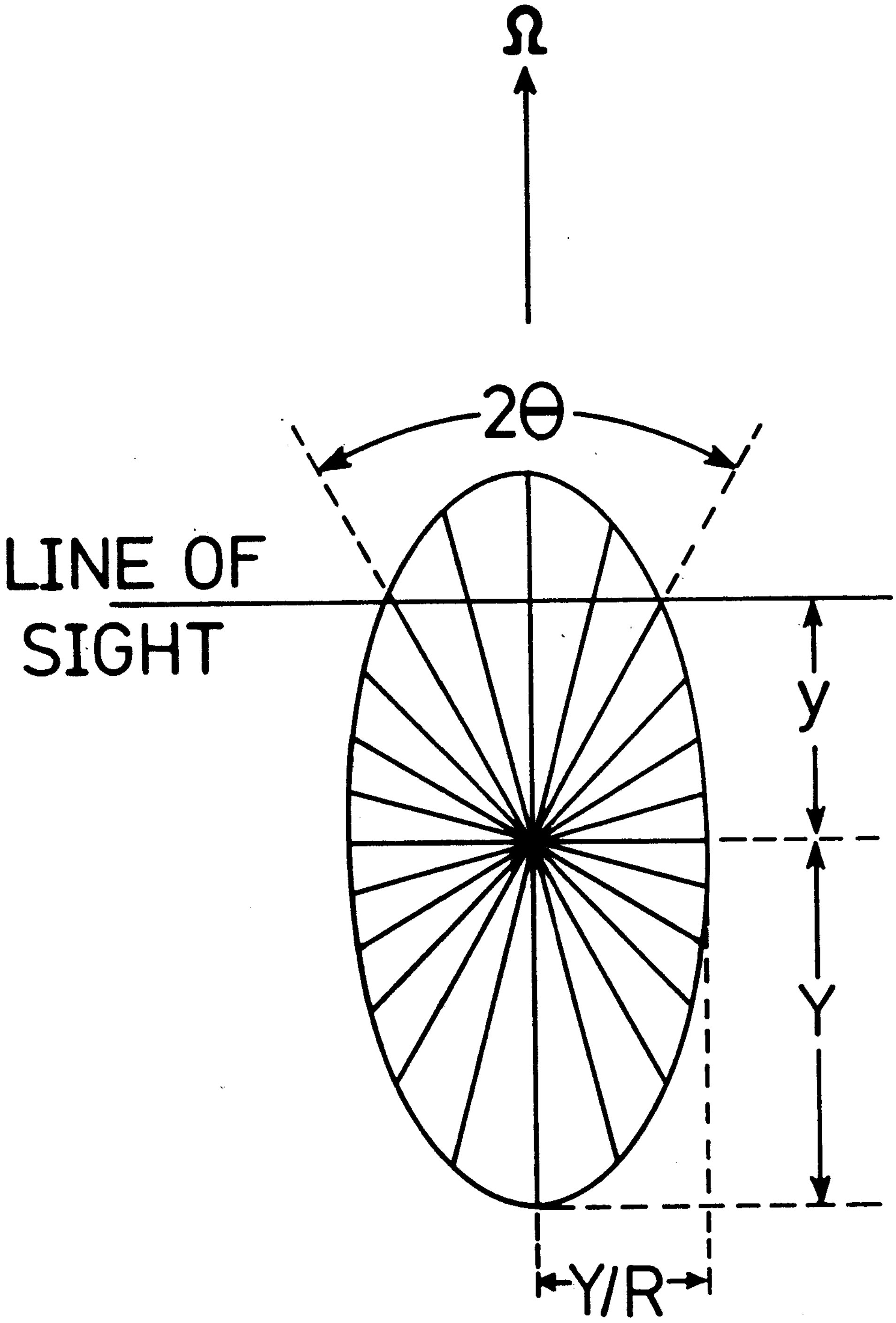

FIG. 6.2 An elliptic pulsar beam similar to Figure 6.1. The beam elongation is characterized by the parameter R, the ratio of the semi-major axis (Y) to the semi-minor axis (Y/R). The beam elongation is along the direction of the local longitude; Ω is the projected direction of the rotation axis. The line of sight goes East-West with respect to the pulsar and is parallel to the minor axis of the beam. For a given R, the polarisation swing 2θ is a monotonic function of the relative offset $|y/Y|$.

$0 \leq |y/y| \leq 1$ (we discuss the error from this approximation in the next section). Let us divide the pulsars into two groups: group A pulsars with $0 \leq |y/y| \leq 0.5$ and group B pulsars with $0.5 \leq |y/y| \leq 1$. From eq. (6.2) the mean value of $\cos\theta$ in these two groups is

$$\langle\cos\theta\rangle_A = \left[(3+R^2)^{1/2}-2\right] / (R-1/R) \qquad (6.3)$$

$$\langle\cos\theta\rangle_B = \left[2R-(3+R^2)^{1/2}\right] / (R-1/R) \qquad (6.4)$$

The mean value of $\cos^2\theta$ is similarly

$$\langle\cos^2\theta\rangle_A = \frac{1}{Q} - \frac{2}{R\,Q^{3/2}}\tan^{-1}\left(\frac{R\,Q^{1/2}}{2}\right) \qquad (6.5)$$

$$\langle\cos^2\theta\rangle_B = \frac{1}{Q} - \frac{2}{R\,Q^{3/2}}\left[\tan^{-1}(R\,Q^{1/2}) - \tan^{-1}\left(\frac{R\,Q^{1/2}}{2}\right)\right] \qquad (6.6)$$

$$Q = 1 - 1/R^2 \qquad (6.7)$$

The variance $\sigma^2_{A,B}$ on the distribution of $\cos\theta$ in groups A and B is given by

$$\sigma^2_{A,B} = \langle\cos^2\theta\rangle_{A,B} - \langle\cos\theta\rangle^2_{A,B} \qquad (6.8)$$

To estimate R from the available data we order the pulsars in decreasing magnitude of the polarisation angle swing 2θ and divide them into two equal groups - high swing and low swing. We can identify the high swing pulsars with group A and the low swing pulsar with group B. The misfit factor

$$S = n\left[\left(\frac{\Delta\langle\cos\theta\rangle_A}{\sigma_A}\right)^2 + \left(\frac{\Delta\langle\cos\theta\rangle_B}{\sigma_B}\right)^2\right], \qquad (6.9)$$

where $\Delta\langle\cos\theta\rangle$ is the difference between the expected values of $\cos\theta$ and the values computed from observations and n is the number of pulsars in group A (or B), is clearly a function only of the assumed R. We estimate R by locating the minimum value of S and determine the 1σ bounds by identifying the points at which $S = S_{min} + 1$.

Since all the results are based on the specific elliptic shape assumed for the beam, this assumption can be checked with the corresponding (10%) pulse widths W_{10}. For an ellipse (of any R), the mean widths in the two groups should satisfy

$$\frac{\langle W_{10}\rangle_A}{\langle W_{10}\rangle_B} = \frac{0.9566\,(2Y/R)}{0.6144\,(2Y/R)} = 1.56 \qquad (6.10)$$

In comparison, a rectangular beam would have $\langle W_{10}\rangle_A / \langle W_{10}\rangle_B = 1$ while a "diamond"-shaped beam would have a ratio of 2.0, these results being again independent of R.

6.3 ESTIMATION OF BEAM ELONGATION

The estimation of 2θ from polarisation observations is generally complicated by the presence of orthogonal radiation modes (Manchester et.al. 1975; Backer et.al. 1976) and the attendent discontinuous flipping of the mean polarisation angle* However, Backer and Rankin (1980) have shown that, when good data are organized in the form of histograms of the polarisation angle at various longitudes across the pulse, it is quite easy to follow the angle variation of a single mode.

We have estimated 2θ for 16 pulsars (at 430 MHz) from the histograms given by Backer and Rankin (1980). We eliminated two pulsars from their work - PSR 1919+21 because they find an unusual polarisation angle variation which is not easily interpreted, and PSR 1541+09 because the polarisation is very weak* For each pulsar we obtained the mean polarisation angle of one of the orthogonal modes as a function of the longitude (in those cases where the other mode is also strong we combined the data on both modes with a suitable constant angle off-set between them). We fitted the observed angle variation to the RC model (Manchester and Taylor 1977; see also chapter 7) and obtained the polarisation angle swings 2θ listed in table 6.1. We note that the accuracy would have been quite adequate even if we had estimated 2θ directly by eye from the published data. For PSR 1237+25 we have taken 2θ to be 175^o (instead of a small angle as suggested by the data of Backer and Rankin 1980) because several other studies (e.g., Bartel et.al. 1982) show that the line of sight to earth passes very close to the magnetic pole.

The pulsars in table 6.1 have been listed in the order of decreasing 2θ and have been classified into two groups, A and B, of eight pulsars each as discussed in the previous section. Table 6.2 shows the mean value of $\cos\theta$ for groups A and B from which we deduce that $R = 3.0 \pm 0.4$. (for a mean East-West full width of $\sim 15^o$, the mean North-South full width is $\sim 45^o$). This is an extremely large and unexpected elongation* We note that circular beams with $R \simeq 1$ are quite clearly ruled out.

Before considering the meaning and consequences of the large estimate of R, it is necessary to discuss the possible sources of error and any selection effects which could invalidate our results* Our analysis assumes a uniform distribution of $|y/Y|$ in the range 0 to 1. Since the pulsar

TABLE 6.1

Data for 16 pulsars obtained from Backer and Rankin (1980). The values of $|y/Y|$ in the fourth column are computed for R=3.0.

GROUP A

PSR	$2\rho^{o}$	M	$\lvert y/Y \rvert$
1237+25	175	15.2	0.02
0525+21	152	20.8	0.08
0301+19	136	18.3	0.13
2020+28	97.2	18.2	0.28
1133+16	89.6	12.1	0.32
0823+26	79.1	10.6	0.38
0834+06	61.4	9.4	0.49
2016+28	58.0	13.8	0.52

CROUP B

PSR	$2\theta^{o}$	W_{10}^{o}	$\lvert Y/Y \rvert$
2303+30	56.2	7.9	0.53
0950+08	51.0	30.6	0.58
0611+22	40.4	14.2	0.68
1929+10	32.7	22.2	0.75
1604-00	27.0	16.9	0.81
1933+16	25.7	12.1	0.83
1944+17	21.6	31.4	0.87
0540+23	21.0	21.8	0.88

TABLE 61 2

Summarized results for pulsars of group A and group B in table 6.1.

	GROUP A	GROUP B
OBSERVED $\langle \cos\theta \rangle$	0.567	0.949
EXPECTED $\langle \cos\theta \rangle$ FOR R=3.0	0.549 ± 0.089	0.951 ± 0.013
EXPECTED $\langle \cos\theta \rangle$ FOR R=1.0	0.250 ± 0.051	0.750 ± 0.051
$\langle W_{10} \rangle^{\circ}$	14.8 ± 3.8	19.6 ± 7.9
COMPUTED $\langle \lvert y/Y \rvert \rangle$ for R=3.0	0.28	0.74
COMPUTED $\langle \lvert y/Y \rvert \rangle$ for R=1.0	0.57	0.95
EXPECTED $\langle \lvert y/Y \rvert \rangle$	0.25 ± 0.05	0.75 ± 0.05
OBSERVED $\langle \cot\theta \rangle$	0,911	3.66
EXPECTED $\langle \cot\theta \rangle$ FOR R=4.8	1.20 ± 0.24	3.60 ± 0.24

luminosity may be expected to vary as a function of $|y/\gamma|$ this cannot be strictly true* Narayan and ViveKanand (1983) in a study of PSR 0950+08 found that the pulse intensity for an outer cut of the beam is significantly less than for an intermediate cut. In chapter 7 we show evidence for a monotonic fall off of radio flux with the latitude offset $|y/\gamma$. We make yet another independent study in section 6.5 which again suggests a falling luminosity. A fall off rather than an increase in the intensity towards the beam edge is also intuitively appealing. When this selection effect is present, smaller values of $|y/\gamma|$ will be over-represented, which tends to increase 2θ and decrease the estimated value of $\langle\cos\theta\rangle_{A,B}$ in the sample. Therefore our estimated value of 3.0 must be lower than the true value of R.

It is possible that the pulse strength does not fall monotonically with increasing $|y/\gamma|$ but peaks at some intermediate value (the "hollow-cone" model of the pulsar beam might suggest this). To first order this is not expected to affect the estimate of R. Also the data shows no evidence for this effect* Firstly the probability of detecting a pulsar should increase with increasing $|y/\gamma|$ for group A and decrease with increasing $|y/\gamma|$ for group B. Consequently, at the optimum value of R (= 3.0), the observed value of $\langle\cos\theta\rangle_A$ should be larger than the expected value while for group B the trend should be the other way. Table 6.2 shows that there is practically no evidence for this* Secondly, the values of $|y/\gamma|$ of the 16 pulsars, computed using the optimum value of R (table 6.1), should peak around $y/\gamma = 0.5$. Again there is no evidence for this. The mean values $|y/\gamma|$ in groups A and B shown in table 6.2 are entirely consistent with the values 0.25 and 0.75 expected for a uniform distribution*

Another point concerns the choice of the pulse width, The 2θ values in tabel 6.1 correspond to the widths W_{10} (10% of peak intensity) which are almost equal to the full pulse widths* One could instead use other measures of widths such as W_{50}, the width corresponding to 50% of the peak intensity, or W_e the equivalent width. Eoth these are smaller than W_{10} and hence lead to smaller values of 2θ. Therefore, using these measures of width would only increase the deduced elongation R beyond our estimate of 3.0.

Finally we consider the error from our assumption of an elliptic shape for the beam. From table 6.2 we see that $\langle W_{10}\rangle_A / \langle W_{10}\rangle_B = 0.76 \pm 0.36$. The expanded data set in section 6.4 also suggest a similar value. This is not consistent with the value of 1.56 expected for an elliptic beam (section 6.2) but agrees with the value 1.0 for a rectangular beam. Now for a rectangular beam of axial ratio R (=North-South dimension/East-West dimension), $\cot\theta$ is uniformly distributed between 0 and R and hence

$$\langle \cot\theta\rangle_A = 0.25R \pm 0.5R/(12n)^{1/2} \tag{6.11}$$

$$\langle \cot\theta\rangle_B = 0.75R \pm 0.5R/(12n)^{1/2} \tag{6.12}$$

From the observed values of $\langle \cot\theta\rangle_{A,B}$ in table 6.2 we conclude that, if the beam has a rectangular rather than an elliptic shape, then $R = 4.8^{+1.1}_{-0.7}$, which is greater than 3.0. The beam may even be "butterfly" shaped in which case R would be still greater,

One other possible source of error in our analysis is the neglect of spherical effects. This is considered in section 6.5 where we show that none of the above conclusions is affected*

From the above discussion it is seen that our estimate of 3.0 for the beam elongation is really a lower bound. The true value must be larger* Jones (1980) analysed pulsar polarisation data by a technique similar to our arguments in section 6.5 and concluded that $R = 2.5^{+1.3}_{-0.7}$ Since he used half-maximum intensity widths W_{50} , which are approximately $0.6W_{10}$ (for the pulsars in table 6.1), the corresponding R from our calculations is 5.0 ± 0.7 . Jones' value would appear to be an underestimate*

Before closing this section, a word of caution is necessary concerning the statistical reliability of our results, We have used 16 observational numbers to estimate R . It would be reassuring if our conclusions could be confirmed by a larger pulsar sample* Meanwhile, considering the fairly tight 1σ limits which we obtain, we believe these results can be accepted with reasonable confidence.

6.4 EVOLUTION OF BEAM ELONGATION

Kundt (1982) made the interesting suggestion that the elongation parameter R could evolve during the life of a pulsar* To investigate this possibility we use an expanded sample of pulsars* In addition to the 16 pulsars of table 6.1

we now add another 13 pulsars for which Manchester and Taylor (1977, tables 2 and 3) quote reliable values of 2θ (at $\sim$ 400 MHz). We also include PSR 0329+54 for which multifrequency observations of Bartel et.al. (1982) clearly indicate that $2\theta \approx 180^\circ$.

Tables 6.3 a, b and c give the data on the above thirty pulsars grouped into three ranges of the period P, the ten pulsars in each range being divided into two groups as before. The values of W_{10} for the new pulsars are from Manchester and Taylor (1981) except for PSR 0531+21 and PSR 1508+55 whose widths were estimated directly from the original observations of Manchester (1971). The values of 2θ for the Backer-Rankin pulsars and PSR 0329+54 correspond to W_{10} The 2θ values for the other 13 pulsars are the estimate of Manchester and Taylor (1977); it is not clear to what width they correspond. Since the Manchester-Taylor estimates of 2θ for most of the Backer-Rankin pulsars agree very well with ours, we presume they have considered either W_{10} itself or something close to it. Barring two pulsars (viz., PSR 0531+21 and PSR 1919+21) for which 2θ is a little uncertain, we believe the data we use here are quite reliable, though not as uniform as the sample in table 6.1.

Using the method described in section 6.2 we obtain the following estimates of R in the three period ranges

$$
\begin{aligned}
R &= 4.9 \pm 0.7 \,, && P \leq 0.388\ \text{s.} \\
&= 2.5 \pm 0.5 \,, && 0.388\ \text{s.} < P \leq 1.2\ \text{s.} \qquad (6.13) \\
&= 1.3 \pm 0.3 \,, && 1.2\ \text{s.} < P
\end{aligned}
$$

TABLE 6.3

TABLE FOR 30 PULSARS, GROUPED INTO THREE PERIOD RANGES OF 10 PULSARS EACH.

(A) $P \leqslant 0.388$ S.

GROUP A						GROUP B					
PSR	P (S.)	$2\theta^{0}$	W_{10}^{0}	$\lvert d\theta/d\varphi\rvert_{max}^{-1}$	TYPE	PSR	P (S.)	$2\theta^{0}$	W_{10}^{0}	$\lvert d\theta/d\varphi\rvert_{max}^{-1}$	TYPE
2020+28	0.3434	97.2	18.2	0.103	C	1929+10	0.2265	32.7	22.2	0.67	S
0833-45	0.0892	85	19.0	0.17	S	1933+16	0.3587	25.7	12.1	0.48	S
1556-44	0.2570	65	19.6	0.11	S	0540+23	0.2460	21.0	21.8	1.00	-
0950+08	0.2531	51.0	30.6	0.50	S	0531+21	0.0331	20	50	1.0	S?
0611+22	0.3349	40.4	14.2	0.33	-	1642-03	0.3876	20	6.6	0.11	S

(B) 0.388 S. $<$ $P \leqslant 1.2$ S.

GROUP A						GROUP B					
PSR	P (S.)	$2\theta^{0}$	W_{10}^{0}	$\lvert d\theta/d\varphi\rvert_{max}^{-1}$	TYPE	PSR	P (S.)	$2\theta^{0}$	W_{10}^{0}	$\lvert d\theta/d\varphi\rvert_{max}^{-1}$	TYPE
0329+54	0.7145	180	16.1	0.036	S?	2016+28	0.5580	58	13.8	0.20	S
1508+55	0.7396	180	12.1	0.053	S?	2021+51	0.5291	50	21.8	0.29	S
1133+16	1.1879	89.6	12.1	0.103	C	1154-62	0.4005	40	27.0	0.50	S
0823+26	0.5307	79.1	10.6	0.071	-	1604-00	0.4218	27.0	16.9	0.59	-
1240-64	0.3884	60	19.5	0.24	S	1944+17	0.4406	21.6	31.4	1.4	-

(C) 1.2 S. $<$ P

GROUP A						GROUP B					
PSR	P (S.)	$2\theta^{0}$	W_{10}^{0}	$\lvert d\theta/d\varphi\rvert_{max}^{-1}$	TYPE	PSR	P (S.)	$2\theta^{0}$	W_{10}^{0}	$\lvert d\theta/d\varphi\rvert_{max}^{-1}$	TYPE
1237+25	1.3824	175	15.2	0.017	C	0628-28	1.2444	90	37.6	0.22	S
0525+21	3.7455	152	20.8	0.033	C	2319+60	2.2564	75	24.7	0.100	C
2045-16	1.9615	145	17.1	0.027	C	0834+06	1.2738	61.4	9.4	0.077	C
0301+19	1.3876	136	18.3	0.056	C	2303+30	1.5759	56.2	7.9	0.13	-
1700-32	1.2117	135	19.0	0.025	S	1919+21	1.3373	25	11.3	0.083	C

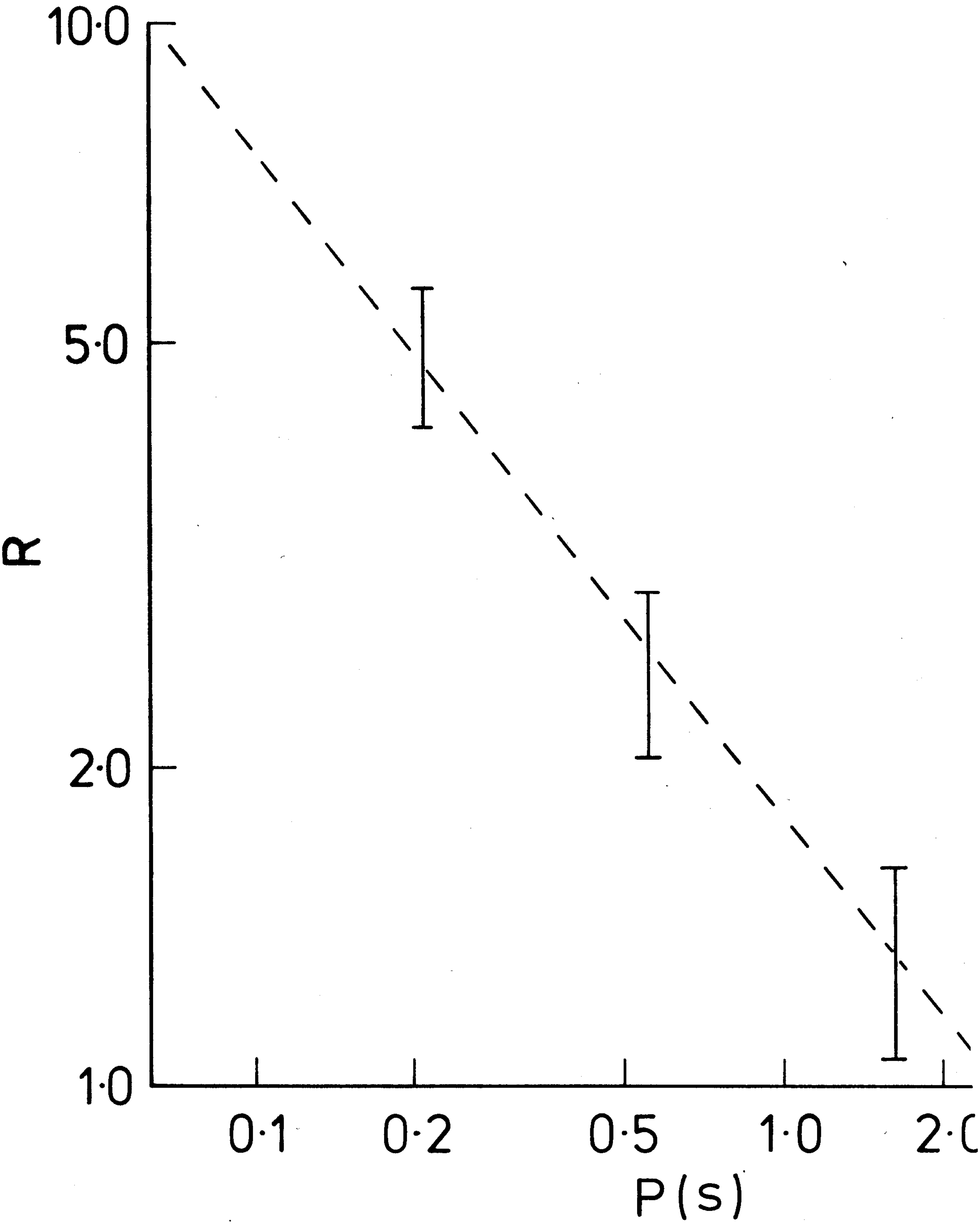

FIG. 6.3 Variation of the elongation parameter R with pulsar period. The estimated R, along with the 1 error limits, are plotted against the geometric-mean periods of the pulsars in the three period ranges discussed in section 6.4. The dashed line is tho visually ostimatod bost fit and corresponds *to* $R=1.8\ P^{-0.63}$

There is virtually no variation of R with $\dot{P}$ while the weak variation with τ and B_{12} is probably due to the variation with P We thus conclude that the beam elongation is primarily a function of the pulsar period and has essentially no dependence on other pulsar parameters*

6.5 SPHERICAL EFFECTS

In the analysis so far we have assumed a planar geometry* In reality the beam is a cross-section of a cone attached to a rotating, spherical neutron star. We now make an analysis including the spherical effects. As might be anticipated the earlier results continue to hold. However, since the analysis here is different and also makes use of a different set of observational data, viz., $|d\theta/d\varphi|_{max}$, it confirms that our picture is internally consistent,

Let α be the angle between the magnetic and rotation axis and β the latitude off-set between the magnetic axis and the line of sight (fig. 6.4). Let β_{max} be the maximum off-set at which the pulsar is visible. Hence the North-South dimension of the beam is $2\beta_{max}$. Let the maximum angular East-West dimension of the beam be Υ_{max} (which corresponds to $2Y/R$ in fig. 6.2). Assuming an elliptic shape for the beam, the East-West dimension $\Upsilon(\beta)$ at any off-set β is given by .

$$\left(\frac{\Upsilon(\beta)}{\Upsilon_{max}}\right)^2 + \left(\frac{\beta}{\beta_{max}}\right)^2 = 1, \qquad |\beta| \leq \beta_{max} \tag{6.16}$$

The pulse width $W_{10}(\beta)$ measured in degrees of longitude is given by

$$W_{10}(\beta) = \frac{\Upsilon(\beta)}{\sin(\alpha+\beta)} \tag{6.17}$$

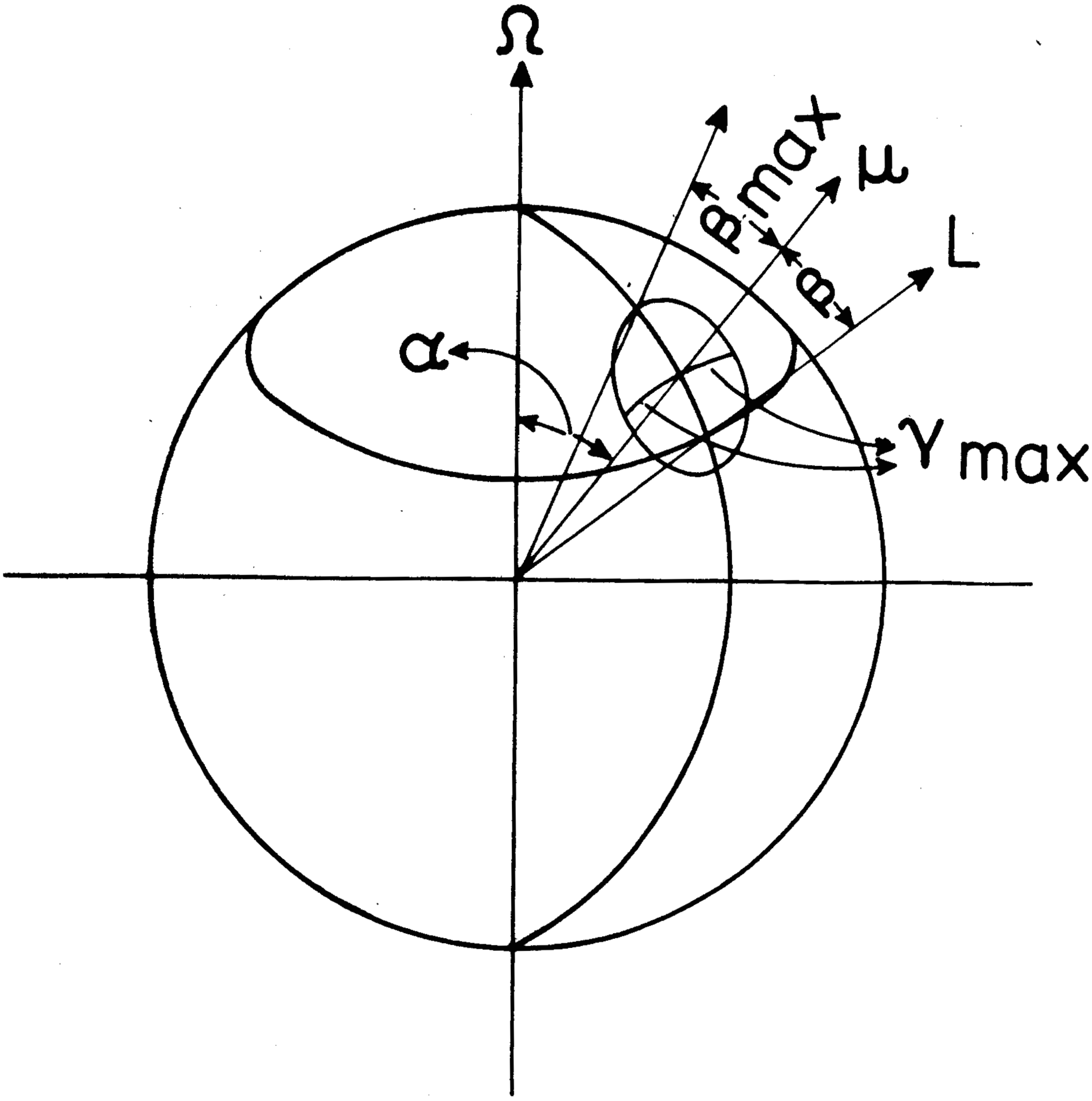

FIG. 6.4 Illustration of the spherical geometry of the pulsar beam. The spherical neutron star spins around the rotation axis Ω. The magnetic dipole moment μ makes an angle a with respect to Ω. The pulsar beam is a cone centred on the magnetic pole, having an elliptic cross-section, with angular axial dimensions $2\beta_{max} \times 2\gamma_{max}$. The line of sight L at a latitude offset β from μ traces a line of constant latitude $\alpha+\beta$.

Using the spherical weighing factor $\frac{1}{2} d\beta \sin(\alpha+\beta)$ for the probability of occurrence of a given off-set between β and $\beta + d\beta$ we calculate the mean pulse width $\langle W_{10}\rangle$ to be

$$\langle W_{10}\rangle = \frac{1}{2P}\int_{-\beta_{max}}^{+\beta_{max}} d\beta \left[\Upsilon(\beta) / \sin(\alpha+\beta)\right] \sin(\alpha+\beta)$$

$$= \frac{\pi\, \Upsilon_{max}\, \beta_{max}}{4 \sin\alpha \sin\beta_{max}} \qquad (6.18)$$

where, taking $\beta_{max} \ll \alpha$ we have

$$P = \frac{1}{2}\int_{-\beta_{max}}^{+\beta_{max}} d\beta \sin(\alpha+\beta) = \sin\alpha \sin\beta_{max} \qquad (6.19)$$

The mean value of $|\sin\beta|$ over all lines of sight is similarly

$$\langle|\sin\beta|\rangle = \frac{1}{2P}\int_{-\beta_{max}}^{+\beta_{max}} d\beta |\sin\beta| \sin(\alpha+\beta) = \frac{1}{2} \sin\beta_{max} \qquad (6.20)$$

In the above results we have not considered the variation of luminosity with $|\beta|$.

Now, the rate of change of polarfsation angle with pulsar longitude $d\theta/d\varphi$ reaches its maximum value when the line of sight is closest to the magnetic pole. At this point we have (Manchester and Taylor, 1977, eq. (10-25))

$$|d\theta/d\varphi|_{max} = \left|\frac{\sin\alpha}{\sin\beta}\right| \qquad (6.21)$$

Combining with equation (6.20) we see that

$$\sin\beta_{max} = 2 \sin\alpha_{eff} \langle |d\theta/d\varphi|^{-1}_{max}\rangle \qquad (6.22)$$

where we have written the equation for an effective α.

Table 6.3a to 6.3c list $|d\theta/d\varphi|^{-1}_{max}$ for all 30 pulsars. For the Backer-Rankin pulsars we have used our least squares fits of polarisation angle variation, while for the others (including

PSR 0329+54 and PSR 1237+25) we used the values of Manchester and Taylor (1977). From eq. (6.22), which makes no assumptions of the beam shape, and assuming α_{eff} to be 60°, we obtain

$$2\beta_{max} = 101^{\circ}{}^{+49^{\circ}}_{-31^{\circ}} , \quad P < 0.388\ s.$$
$$= 74^{\circ}{}^{+37^{\circ}}_{-30^{\circ}} , \quad 0.388\ s. \leq P < 1.2\ s. \quad (6.23)$$
$$= 15^{\circ}{}^{+4^{\circ}}_{-4^{\circ}} , \quad 1.2\ s < P$$

Although the analysis made here is not as sensitive as the methods of earlier sections, we note that the rapid evolution of the North-South beam dimension with period persists* Moreover, by the structure of eq. (6.22) it is clear that the actual value of α_{eff} that we assume is unimportant as far as the variation of β_{max} is concerned, Also the above analysis does not make any assumption on the beam shape,

Using eq. (6.18), which is valid for an elliptic beam, we can estimate γ_{max} from W_{10} , The beamelongation is then given by

$$R = 2\beta_{max} / \gamma_{max} \quad (6.24)$$

Figure 6.5 shows the variation of (deduced) R with α_{eff} in the three period ranges* Since R is seen to be insensitive to α_{eff}' the evolution of beam elongation with period cannot be explained by invoking a period evolution of α_{eff} .

Finally, we consider the variation of luminosity with $|\beta|$, Let us divide the pulsars in each of the tables 6.3a to 6.3c into two groups - group A' containing the five pulsars with

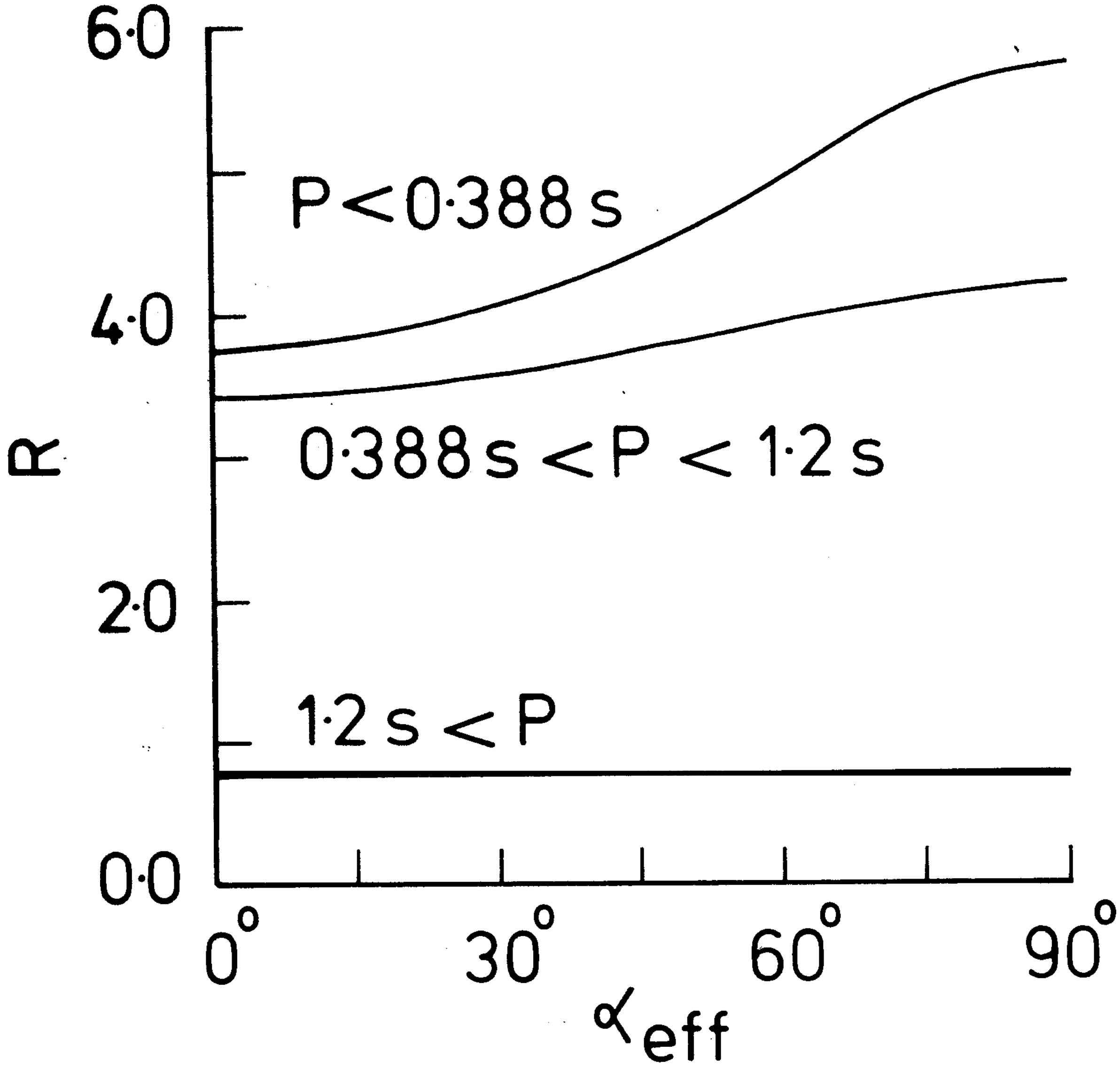

FIG. 6.5 Variation of the estimated beam elongation R with the mean angle α_{eff} between the rotation and magnetic axes. It is reasonable to expect that $30^o < \alpha_{eff} < 60^o$. Note that R is fairly insensitive to α_{eff} in all the three period ranges. The actual values of R shown here are different from (but statistically consistent with) those in Figure 6.3 because the method of analysis as well as the data used are not the same.

the lowest values of $|d\theta/d\varphi|^{-1}_{max}$, and group B' having the five pulsars with the highest values of $|d\theta/d\varphi|^{-1}_{max}$ (these groups are evidently different from the earlier groups A and B). A comparison of eqs. (6.19) and (6.22) shows that for a given , if there is no luminosity selection effect, the mean value of $|d\theta/d\varphi|^{-1}_{max}$ over the range 0 to any β is directly proportional to the corresponding probability . Thus $|d\theta/d\varphi|^{-1}_{max}$ is uniformly distributed between 0 and $\frac{\sin\beta_{max}}{2\sin\alpha_{eff}}$. Therefore

$$K = \frac{\langle|d\theta/d\varphi|^{-1}_{m}\rangle_{B'}}{\langle|d\theta/d\varphi|^{-1}_{m}\rangle_{A'}} = \frac{0.75(\sin\beta_m/2\sin\alpha_{eff})}{0.25(\sin\beta_m/2\sin\alpha_{eff})} = 3.0 \qquad (6.25)$$

From the data in tables 6.3a to 6.3c we estimate K to be 4.4 ± 4 6.6 ± 3.0, and 4.0 ± 1,2 in the three period ranges, leading to a weighted mean value

$$K = 4.4 \pm 0.9 \qquad (6.26)$$

A value of $K > 3$ implies that there is a crowding of lines of sight close to the magnetic pole and a spreading out farther away, Thus we find that the beam luminosity in pulsars falls with increasing $|\beta|$. This agrees with other, independent studies (Narayan and Vivekanand 1982,1983). The value 4.4 for is consistent with the .value 3.9 expected for a Gaussian variation, though other forms are also possible (for instance, K =5.5 for an exponential variation and 3.8 for a triangular fall-off). However, the analysis made here virtually rules out any question of luminosity increase outwards from the magnetic pole, which, as discussed in section 6.1 is the only way to reconcile the polarisation data with a circular beam.

CHAPTER 7

RELATIVE ORIENTATION OF $\vec{\Omega}$, AND $\vec{L}$

7.1 INTRODUCTION

In the previous chapter we derived the important result that the cross-section of pulsar beams is actually elongated, and not circular, and that the elongation decreases with increasing period, Given the dimensions of pulsar beams, we can compute the beaming fraction provided we know the allowed relative orientations of the rotation axis, the magnetic axis and the line of sight* In the context of the RC model (Radhakrishnan and Cooke 1969), two angles α and β (Fig. 7.1) decscribe the pulsar geometry. In this chapter we estimate the' values of these angles for a number of individual pulsars by analysing the available polarisation data (mostly from Backer and Rankin (1980); henceforth BR). In particular we investigate the distribution of α and the sign of β , because this information is essential to compute the beaming fraction f .

There have been very few attempts to estimate these angles observationally. Radhakrishnan and Cooke (1969) used polarisation information to place, upper bounds on α and β for PSR 0833-45 ($\alpha < 50^o$; $\beta < 10^o$) and also suggested

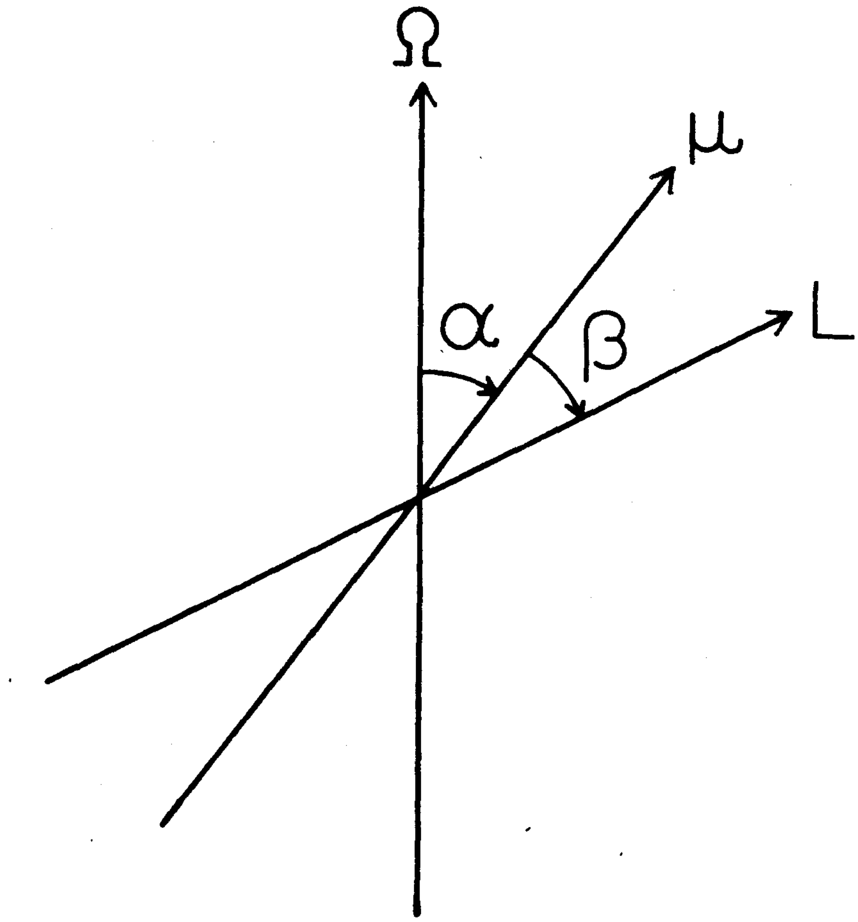

FIG. 7.1 Ω , μ and L are the direction of the rotation axis, magnetic axis and line of sight at an instant when all three are in the same plane. The angles a and β are considered positive in the direction away from the rotation pole. Positive and negative β are called outer and inner lines of sight respectively.

that $\beta < 0^\circ$ for PSR 0531+21 (for this pulsar $\alpha \sim 90^\circ$ bacause of the interpulse). Manchester and Taylor (1977, henceforth MT) made least squares fits of the observed polarisation angle variation in four pulsars and gave estimates of β (the quality of the data did not permit simultaneous estimation of α and β ; therefore they assumed a mean value of 60° for α) More recently, Narayan and Vivekanand (1983) proposed a model for PSR 0950+08 using the polarisation data of BR (1980) in which they use $\alpha = 10^\circ$ and $= -5^\circ$. Apart from these, the only other pulsar where some information is available on the beam geometry is the binary pulsar PSR 1913+16, where, if one assumes that the rotation axis is normal to the plane of the orbit, one deduces that $\alpha + \beta = i = 47^\circ$ (Taylor 1980).

We use three essentially independent arguments, all based on the RC model, and these are presented separately (methods A, B and C). Our discussion makes use of the following: (a) In the RC model, when the magnetic field lines are projected on the star surface, they form great circles passing through the magnetic poles. (b) The line of sight traces a small circle of constant "latitude" $90^\circ - \alpha - \beta$ (referred to the rotation axis) and the polarisation angle at any longitude is the angle at the corresponding point on the surface of the star between the local magnetic great circle and the line of sight small circle. (c) From (a) and (b), it can be shown (MT) that the gradient of the polarisation angle θ with respect to φ at the centre of the pulse (i.e., the point of closest approach to the magnetic pole) is given by

$$\left| d\theta / d\varphi \right|_{central} = \left| \frac{\sin \alpha}{\sin \beta} \right| \qquad (7.1)$$

The actual sign of $d\theta/d\varphi$ has no useful information for our present purposes.

7.2 METHOD A

From eq. (7.1) it is seen that the value of $|d\theta/d\varphi|$ gives $|\beta|$ as a function of α, but does not determine the actual values of α and β, nor even the sign of β (for exceptions see method B below). However the detailed shape of the curve, which is given by (MT),

$$\tan\theta = \frac{\sin\alpha\sin\varphi}{\cos\alpha\cos(\alpha+\beta) - \sin\alpha\cos(\alpha+\beta)\cos\varphi} \qquad (7.2)$$

has much more information than the central gradient (fig. 7.2 shows typical examples). A striking characteristic of the θ-φ curve for positive β (we call this an "outer" line of sight since $\vec{L}$ lies outside the angle formed by $\vec{\Omega}$ and $\vec{\mu}$, fig. 7.1) is its flattening as one moves away from the pulse centre, with a ,maximum polarisation swing less than 180^o, On the other hand, the θ-φ curve for negative β ("inner" lines of sight) is monotonic, Figure 7.2 shows that the difference between the curves for $+\beta$ and $-\beta$ at a given pulse longitude increases as α decreases* Because of. these effects, given accurate observations of θ as a function of φ, it is possible to estimate α and β by means of curve fitting procedures.

Table 7.1 shows the results we obtain by least squares fits on the excel lent data of BR (it is because of the improved data that we get tighter estimates on α and β than MT). For

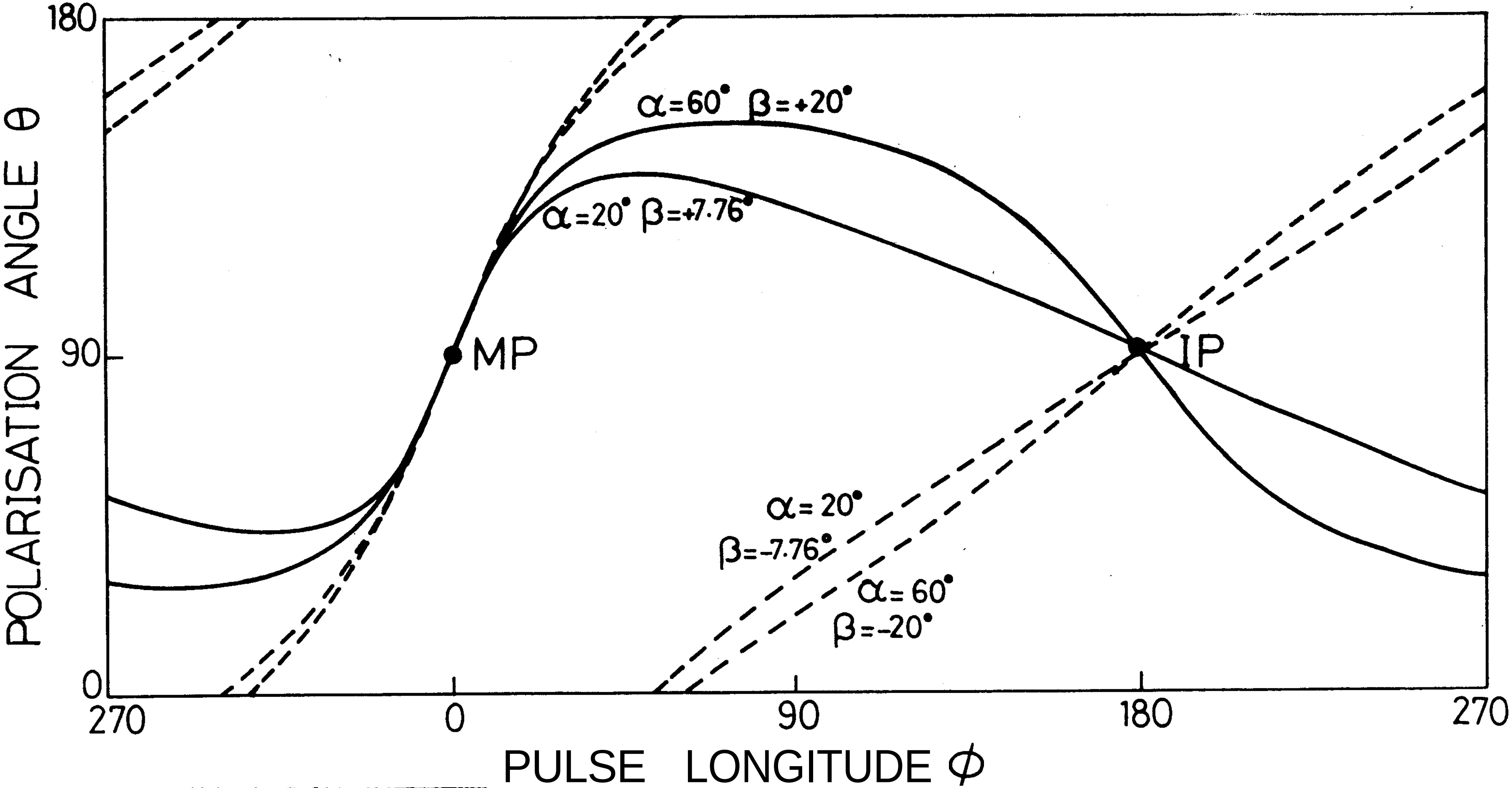

FIG. 7.2 Variation of polarisation angle 8 across 360^{o} of pulse longitude ⊧ . The solid lines correspond to positive β and the dashed lines to negative B . The points MP and IP are the centres of the main and inter pulses. All the four curves have the same value of $d\theta/d\phi$ at MP, but deviate from one another away from this point. Note (a) the topological distinction between positive and negative curves, (b) the increased difference between positive and negative β curves at small values of a for the same value of $(d\theta/d\phi)_{MP}$, and (c) the opposite slopes of solid and dashed lines at the interpulse.

TABLE 7.1

Estimates of α and β of seven pulsars, obtained by least square fits of the data of BR (method A). Values in parentheses are doubtful because of the relativly larger r.m.s. residuals. Where limits are given on α, the value of β corresponds to the extreme value of α.

PSR	α	β	probability (%) of $+\beta$	probability (%) of $-\beta$	residual in θ
0301+19	$70^\circ \pm 11^\circ$	$+3.0^\circ$	97%	3%	1.0°
0525+21	$\leq 20^\circ$	$+0.6^\circ$	100%	0%	1.4°
0950+08[a]	$\leq 25^\circ$	-12°	0%	100%	3.8°
1133+16	$(90^\circ \pm 60^\circ)$	$(+6.0^\circ)$	(50%)	(50%)	1.7°
1929+10	$50^\circ \pm 61^\circ$	$+32^\circ$	69%	31%	0.7°
2016+28	$\leq 30^\circ$	$+5.7^\circ$	100%	0%	1.4°
2020+28	$(\leq 25^\circ)$	$(+2.9^\circ)$	(100%)	(0%)	2.1°

a
Values taken from NV. The r.m.s. error in θ is larger because the whole data, including the interpulse, have been fitted, and not just the most accurate data as in other cases. Similar values of α and β are obtained even if the main pulse data alone are considered.

each pulsar we have computed the mean observed θ as a function of the pulse longitude from the published histograms, applying the relavent off-sets (estimated from the data) in the case of orthogonal polarisation modes (this procedure was discussed in the chapter 6). In order to include only the most reliable data, we have retained only those longitudes where BR could estimate the polarisation angle in at least 15% of the pulses (these lonqitudes are labelled "2" or better in the second last column marked "A" in their histograms). Table 7.1 gives our estimates of α and β for seven pulsars. For each pulsar we obtain the best positive β fit as well as the best negative β fit. By using the standard statistical technique of comparing the residuals in the two cases, we can infer the relative likelihood of occurrence of the two cases. These probabilities have been tabulated in table 7.1. In the rest of BR's pulsars the parameters are too poorly determined to be of interest. The last column in table 7.1 gives the r.m.s. difference between the observed and fitted polarisation angles* We estimate that our procedure of computing values of θ from BR's histograms has contributed an r.m.s. error of about 0.5^o to 1.0^o, We therefore consider the results of table 7.1 to be quite reliable for the four pulsars with a final r.m.s. of less than 1.5^o. The results on PSR 1133+16 are probably sound while those on PSR 2020+28 are much less certain* Pulsar 0950+08 has been studied separately by Narayan and Vivekanand (1983) and their results quoted here are statistically quite reliable,

7.3 METHOD B

Since $|\beta|$ cannot be less than α (see fig. 7.1), eq. (7.1) shows that $\left|\frac{d\theta}{d\varphi}\right|_{central} > 1.0$ for inner lines of sight. Thus any pulsar with a gradient less than 1.0 must have positive β. Moreover, if we assume equal emission from both magnetic poles, then we have the obvious inequality $\alpha + \beta < 90^{\circ}$ for the main pulse. Combining these results we can place rigorous upper limits on α for pulsars having $\left|\frac{d\theta}{d\varphi}\right|_{central} < 1.0$. Table 7.2 shows four such pulsars among those observed by BR. The values of the gradient were computed by least squares fits on the histograms of BR using all data corresponding to the symbol "+" or better. Two of the four pulsars, viz. PSR 1237+25 and PSR 1541+09, display very unusual $\theta - \varphi$ curves, not consistent with the RC model; this is reflected in the large residuals, However, the results on PSR 0540+23 and PSN 1944+17 are quite unambiguous and imply positive values of β (outer lines of sight) and the upper limits on α shown in table 7.2.

7.4 METHOD C

Figure 7.2 shows that the polarisation angle gradient in the interpulse has the same sign as that of the main pulse for negative β and the opposite sign for positive β. This is therefore a very straightforward technique of determining the sign of β (RC 1969; see also Hankins and Cordes 1980). Thus, in table 7.3, of the five pulsars with polarisation observations on both mainpulse and interpulse, three have inner

TABLE 7.2

Limits on α for four pulsars estimated by means of method B. These pulsars have positive values of β (equal to $90^\circ - \alpha$ for the extreme value of α). Values in parentheses are doubtful because of the relatively large r.m.s. values.

PSR	$\left\lvert \frac{d\theta}{d\varphi} \right\rvert$ [a]	α	residual in θ
0540+23	0.97 ± 0.05	$\leq 44^\circ$	1.1°
1237+25	(0.64 ± 0.12)	($\leq 33^\circ$)	4.3°
1541+09	(0.46 ± 0.04)	($\leq 25^\circ$)	4.8°
1944+17	0.68 ± 0.03	$\leq 35^\circ$	1.7°

[a] Obtained by least squares straight line fits on the data of BR.

lines of sight (negative β) and two have outer (positive β). If we now assume that the interpulse corresponds to the point of closest approach to the second magnetic pole, then we have

$$(d\theta/d\varphi)_{interpulse} = \frac{-\sin\alpha}{\sin(2\alpha+\beta)} \qquad (7.3)$$

where the gradient of the main pulse has been taken to be positive and is positive or negative as the case may be. Equation (7.3) is correct even if the radiation in the interpulse comes from the same pole as the main pulse. Using eq. (7.1) and eq. (7.3) and the observed polarisation angle gradients at the mainpulse and the interpulse, it is possible to estimate both α and β . The results are given in table 7.3. For PSR 0531+21 we confirm the results of RC who estimated that $\alpha \sim 90^{o}$ and $\beta < 0^{o}$. In the case of PSR 1055-52, the magnitude of the interpulse gradient is not clear and hence our estimates of α and $|\beta|$ are in considerable doubt. The negative sign of β is however quite unambiguous,

7.5 CONCLUSIONS

From the summarized results of tables 7.1,7.2 and 7.3 we conclude the following:

(a) Pulsars 0950+08 and 1929+10 have been analysed by two methods, viz., A and C. Tables 7.1 and 7.3 show that in both cases the results are consistent, confirming the validity of the arguments used,

TABLE 7.3

Values of α and β for five pulsars estimated using method C. Values in parentheses are doubtful because the interpulse gradient is ambiguous.

PSR	$(d\theta/d\varphi)_{central}$		α	β		$\left\lvert \frac{\beta_{IP}}{\beta_{MP}} \right\rvert$	flux ratio S_{IP}/S_{MP} [a]
	main pulse	inter pulse		main pulse	inter pulse		
0531+21	6.0 [b]	+3.1 [b]	86°	-9.6°	+18°	1.8	0.36
0823+26	14.3 [c]	-4.6 [d]	82°	+4.0°	+12°	3.0	0.005
0950+08	2.0 [e]	+0.67 [e]	10°	-5.0°	-15°	3.0	0.018
1055-52	1.6 [f]	(+2.1 [f])	(95°)	(+38°)	(-28°)	(0.74)	(0.85)
		(+0.66 [g])	(20°)	(-12°)	(-28°)	(2.3)	(0.85)
1929+19	1.48 [c]	-0.58 [d]	35°	+23°	+87°	3.8	0.02

a Taken from Manchester and Taylor (1977).
b From the fit of Kristian et al. (1971) on optical data.
c Least squares fit on the data of BR.
d From Rankin and Benson (1981).
e From NV.
f From Fig. 12 of McCulloch et al. (1978).
g From Fig. 3 of McCulloch et al. (1976).

(b) There is clear evidence for the occurrence of both inner and outer lines of sight. We note in particular that positive β values have been deduced using all three independent arguments A, B and C. Therefore, given the RC model, outer lines of sight are quite inescapable, The theory of pulsar electrodynamics developed by Arons and others (e.g.,Arons 1979), which makes a clear prediction that only negative values of are allowed, needs to be reconsidered.

(c) Table 7.1 shows a preponderance of pulsars with positive β . A partial explanation could be that the least squares works best in those pulsars having small values of α ; a positive β is then more likely than negative β on solid angle considerations. Alternatively, it is possible that there could be some systematic distortion of the (assumed) radial field lines leading to a $\theta-\varphi$ curve similar to that expected (in the RC model) for small values of α and positive β (fig. 7.2). If so, theresultsof table 7.1 may be in doubt.

(d) The various reliable indications in tables 7.1, 7.2 and 7.3 give the magnitude of $\langle|\beta|\rangle$ (including interpulses) to be $\sim 22^{o}$ (we have used the maximum value of β where only upper limits are available; this will tend to increase our estimate of $\langle|\beta|\rangle$) This gives a beam size of $|\beta_{max}| \sim 44^{o}$ which is consistent with 22^{o} estimated in the previous chapter* However, there appears to be a preponderence of small values of β , whereas one expects a uniform distribution upto β_{max} This could mean that the apparent luminosity falls off with increasing $|\beta|$ (also see argument (f) below). Alternatively, it might be a consequence of many of the β values being upper bounds.

(e) The values of α that we have estimated appear to be generally rather small, This can be partly accounted for by the fact that methods A abd B both work best at small α (method C, on the other hand, prefers large α) However, even after allowing for this, there seems to be a residual preference for small α . For example, of the total of 18 pulsars observed by BR, five pulsars (viz., PSRs 0525+21, 0950+08, 1929+10, 1944+17, and 2016+28) have $\alpha \lesssim 35^{\circ}$. Even if none of the other 13 pulsars has $\alpha \lesssim 35^{o}$,, this is still more than the 1.9 pulsars expected for a random distribution of α and β (with $|\beta_{max}| \sim 22^{\circ}$). Our result might mean that pulsars work better at small values of α . Alternatively, one could propose that the pulsar magnetic axis aligns with the rotatiion axis with age (as suggested by Goldreich 1970). However, we feel that this is unlikely since the estimated ages ($\simeq \frac{1}{2} P/\dot{P}$) of the pulsars with small d are not significantly different from the others in the BR sample. Moreover, four out of the five pulsars with $\alpha \lesssim 35^{\circ}$ have periods shorter than the average.

(f) The three pulsars in table 7.3 with very weak radio interpulses have $|\beta_{interpulse}/\beta_{mainpulse}| \sim 3.0$. On the other hand, PSR 0531+21 with a β ratio of 1.8 has a fairly strong interpulse. Thus there seems to be some evidence for a monotonic fall off of the radio flux with the latitude off-set β between the magnetic pole and the line of sight, The limited data in table 7.3 suggest the integrated pulse strehgth varies approximately as $|\beta|^{-3}$.